16th World Conference on Earthquake, 16WCEE 2017

Santiago Chile, January 9th to 13th 2017

Paper N°1306

Registration Code: S-C1464733306

Numerical Modeling of Self-Centering Steel Plate Shear Walls

X.Y. Wang(1), W.S. Lu(2), J.P. Han(3)

(1) *Ph. D. candidate, College of Civil Engineering, Tongji University, Shanghai, China. E-mail: wxyjennifer@163.com*
(2) *Professor, College of Civil Engineering, Tongji University, Shanghai, China. E-mail: wally@tongji.edu*
(3) *Professor, School of Civil Engineering, Lanzhou University of Technology, China. E-mail: jphan@lut.cn*

Abstract

The self-centering steel plate shear wall (SC-SPSW) system is a new seismic load-resisting system that combines the steel plate shear wall (SPSW) and the post-tensioned (PT) beam-to-column connection. It has strong lateral load resistance, high energy dissipation and good recentering capability. Numerical model proposed in this research is for capturing the detailed behaviors of SC-SPSW and investigating the effects of various parameters on web plate and PT connection behaviors. The seismic responses including hysteresis response, the PT connection forces and the web plate shear resistance were compared with the experimental data to validate the modeling method. The results present a good agreement in the system performance and the numerical model is able to account for web plate tension field action including the web plate stress and strain variation. This study proves that the thicker web plate increases the PT boundary frame demands and decreases the system recentering capability. With the increasing web plate thickness, the compressive stress in web plate also increases. Furthermore, the compressive stress has an increasing trend after the web plate full yielding under the cyclic load. The research provides an effective modeling method for the parametric study of the SC-SPSW performance.

Keywords: self-centering; web plate; PT connection; numerical model; compressive stress

1. Introduction

Self-centering steel plate shear wall (SC-SPSW) system is a steel frame that features thin steel infill plates and posttensioned (PT) connections between the horizontal boundary elements (HBEs) and vertical boundary elements (VBEs), as shown in Fig. 1 [1]. The steel infill plates, referred to as web plates, are allowed to buckle in shear and develop tension field action under lateral loading. These web plates provide significant stiffness, strength, and energy dissipation. The PT connections, in Fig.1(b), consists of PT tendons spanning the length of the HBE and anchored at the outer flanges of the VBEs. This kind of connection allows a joint gap opening to form between the VBE and HBE interface about a rocking point, leading to a PT elongation, recentering the system, shown schematically in Fig. 1(c). SC-SPSW is intended to reduce residual drift and structure damage to the boundary frame and reduce repair costs and loss of functionality in a building after an earthquake. The structural properties of SC-SPSW make it especially attractive in high seismic regions.

For a SC-SPSW system, the idealized cyclic hysteretic response is shown in Fig. 2. The total hysteretic response of a SC-SPSW is provided by the combined elastic response of the PT boundary frame and the inelastic energy dissipation of the web plate. Assuming the web plates yield in an elastic-perfectly plastic manner. The PT connection is initially compressed by the initial PT force, T_0, the connection gap opening forms at the decompression moment, M_d. So the combined system retains the high initial stiffness and strength of the web plate, and shows bilinear elastic response of the PT boundary frame when combined with the inelastic hysteretic response of the energy dissipation elements that provides the characteristic “flag-shaped” hysteretic response of self-centering lateral force-resisting systems. Upon unloading, the PT provides a restoring force and recentering stiffness that closes the HBE-to-VBE joint gap, and is equal to the post decompression stiffness of the PT connections. In subsequent cycles, the system retains the strength and stiffness contributions of the PT connections until the plates reach their previous peak plastic strain where they again contribute significant strength and stiffness to the system.

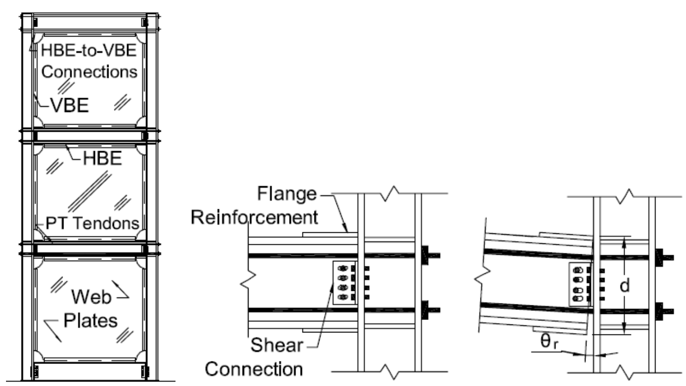

Fig. 1 – (a) Typical SC-SPSW elevation; (b) PT connection detail; (c) decompressed connection[1]

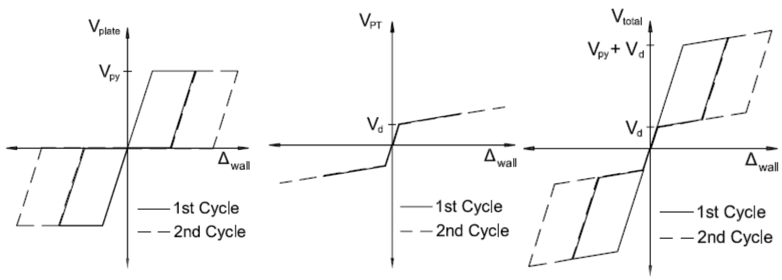

(a) SPSW response (b) PT response (c) SC-SPSW response

Fig. 2 – System force-displacement idealized responses[1]

The research on SC-SPSW started from the project NEES-SG: Smart and Resilient Steel Plate Shear Walls for Reducing Earthquake Impacts. A group of researchers have investigated the design philosophies [1, 2, 3] and done the experimental and numerical simulation study of SC-SPSW. The experiments consist of three phases: large-scale quasi-static subassembly tests， third-scale quasi-static and shaking table tests and full-scale pseudo-dynamic tests [4, 5, 6]. To understand the overall system behavior of SC-SPSW, the quasi-static subassembly experiments are clearly described in [4], which including four, two-story specimens and investigated the impact on response of two parameters: the number of post-tensioning strands used in PT connection, and the web plate thickness. With regard to the numerical studies, Clayton et al. have presented different methods of modeling SC-SPSWs [7]. The strip models in OpenSees, employed nonlinear springs in the PT connection to simulate the rocking behavior and a diagonal strip model to simulate the web plate, were primarily investigated, as the tension-compression strip model was shown to better at predicting the reloading and unloading strengths of the SC-SPSWs [8, 9, 10]. However, when it is necessary to research the complex behavior of the web plate, the shell element web plate model is more appropriate to utilize.

To investigate the web plate behavior that can't be captured in the experiments and to provide a modeling method for the future parametric study of the web plate, the focus of this paper is to develop a SC-SPSW modeling method in ABAQUS. According to the quasi-static subassembly tests, the four specimens are modeled and analyzed under monotonic load and cyclic load. The system general response, PT connection and web plate responses of the models are compared with the experimental results for evaluating the modeling method. Furthermore, the detailed behavior of the SC-SPSW, including the PT force, the PT connection moment and the stress and strain developments of the tension field action in web plate, are significantly explained.

2. Description of Model

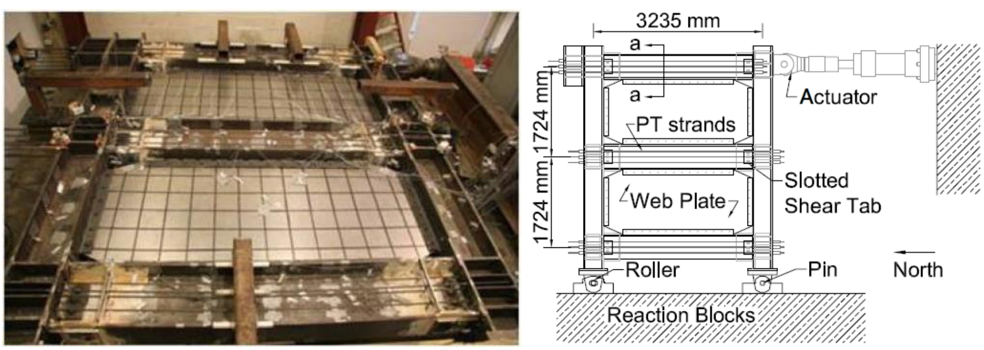

Fig. 3 – (a) Photograph and (b) schematic drawing of the SC-SPSW subassembly test setup[5]

In the first phase of the SC-SPSW experimental program, various large-scale quasi-static subassembly tests were done by Clayton et al. to study the interaction of the PT connection and the web plate and to investigate the effects of various design parameters on the system response. A photograph and a schematic of the test setup are shown in Figs. 3(a) and 3(b), respectively [5]. The SC-SPSW subassembly measured 3,235 mm wide (centerline VBE dimension), with story heights (HBE centerline dimensions) of 1,724 mm. The actuator loaded the specimen at a height of 4,178 mm above the center of the pinned base. The south VBE was pinned at its base to allow for column rotation. Owing to the HBEs rocking about their flanges, as a gap forms in the connections, the VBEs spread apart, this phenomenon is denoted as frame expansion in [11]. A roller under the north VBE was used to accommodate this frame expansion. The test program included variations in the web plate thickness, t_w, number of PT strands, N_s, and initial PT force at each HBE, T_0. There were 5 specimens in the test, named 8s100k, 6s75k20Ga, 8s100k20Ga, 6s75k16Ga and 8s100k16Ga, respectively. The naming scheme identifies the number of strands used in each PT connection (6s or 8s), the initial PT force in units of kips (75k or 100k), and the web plate gauge thickness (16Ga or 20Ga). Test of specimen 8s100k which is without any web plates was done to ensure that the bare PT frame exhibited the desired nonlinear, elastic response. Further details about the test can be found in [4, 5].

Here, except for the bare PT frame, the specimens with in-filled thin steel plate walls are modeled to verify the modeling method. Identical with the test setup, the south VBE was pinned and the north VBE base was constrained by roller at the base through constraining the reference points. The overall model of one specimen is shown in Fig. 4. In these models, solid elements were used to simulate the boundary frame elements, truss elements were used to simulate the PT strands, and S4R shell elements were used to simulate the web plates. All of the beams were connected to the columns by PT connection models. Tie constraints were used to connect the edge of the web plate to the boundary elements. The web plates above and below the middle HBE were same thick for each model.

In the PT connection model, contact interactions between the HBE end flanges and the VBE flange face were employed to simulate the PT connection rocking behavior, rough and hard contact behaviors were defined to allow the interfaces to separate. The slot connector similar to the horizontally-slotted holes used in the shear tab connections at the beam ends, was built to transfer shear forces in the PT beam-to-column connections while allowing the connection to rock open. The PT members were modeled as truss elements that align with the centroid of each PT group on each side of the beam web and the initial stress was loaded by defining the predefined field of temperature. The model also included the continuity and reinforcement plates that were presented in the test specimen. The boundary frame members and reinforcing plates were modeled using solid elements with edge lengths of approximately 50 mm. Also, out-of-plane constraint was provided along the length of each HBE such that only in plane movement of the model occurs.

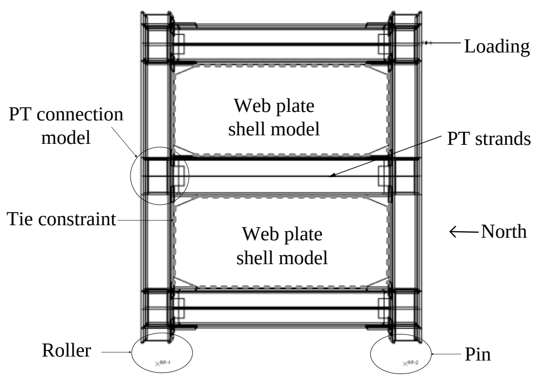

Fig. 4 – SC-SPSW model

Because the boundary elements and PT strands are designed to remain elastic, the boundary frame and the PT strands were modeled using the elastic materials with the elastic moduli 200 Gpa and 196.5 Gpa, respectively. The web plate was defined approximately using elastic-perfectly plastic material model according to the stress-strain curves in the coupon tests in [4], and pure isotropic hardening was used to define the web plate hardening property according to Webster's previous study [12]. As the initial geometric imperfection of the web plate has influence on its behavior, the web plate shell elements were seeded with small initial out-of-plane imperfections from a buckling analysis, with approximate peak amplitudes of 2.8 mm. The web plate was meshed to elements approximately 50×50 mm. To accurately capture inelastic out-of-plane bending behavior of web plate, nine Gauss integration points were used through the thickness of the shell.

For each specimen, the numerical analyses were performed including pushover analysis and cyclic analysis. All of the simulations employed explicit dynamic analysis in ABAQUS/Explicit. Loads were applied using displacement control of a reference point coupling with some area of the column face. The maximum monotonic displacement reached to 4% drift. The displacement amplitude history of the cyclic loading comprised cycles at target peak drifts of 0.117% ($1/3\delta_y$), 0.233% ($2/3\delta_y$), 0.35% (δ_y), 0.7% ($2\delta_y$), 1.05% ($3\delta_y$), 1.5%, 2%, 2.5%, 3%, and up to 4%. δ_y is corresponding to the yield deformation of the specimen.

3. Comparison of Responses

3.1 General response

From the previous description of the SC-SPSW cyclic hysteretic response, the SC-SPSW response is theoretically characterized by the PT connection decompression and web plate yielding. Take model 8s100k20Ga as example, the key characteristics in its push-over and cyclic responses are illustrated in Fig. 5. The red line is the force-displacement curve of specimen 8s100k. Point A corresponds to decompression at the PT connection. As the moment at the connection surpasses the decompression moment, a gap opens on the tension side of the HBE and the PT connection rocks. The stiffness between Points A and B is provided by the elastic tension field in the web plate and the post-decompression stiffness of the PT frame. Point B identifies full yielding of the web plates. From this point on the lateral stiffness will be primarily provided by the post decompression stiffness of the PT frame and strain hardening in the web plates. This is the onset of energy dissipation by the web plates. Noted that the hysteretic curves don't have strength degradation phase due to damage in the web plates are not simulated in the models. In the hysterestic curve, points C through F also can be identified. Point C identifies unloading of the web plate tension field and marks the onset of web resistance via compression and shear. The web plate compressive and shear strength results from plastic deformation and kinking of the web plate and the associated geometric stiffness and strength. Point D indicates the development of the full compressive or shear strength of the plate. Point E indicates the recompression of the PT connection. Point F identifies redevelopment of tension field strength during re-loading following cycles of web plate yielding. In addition to that the bare frame curve can help identify two significant points (Point A and Point C), after the PT connection decompression, the portion of the SC-SPSW hysteretic curve above the bare frame response approximately represents web plate contribution due to the tension field, and the portion of the hysteretic curve below the bare frame response represents the contribution of the compressive strength of the web plate [4].

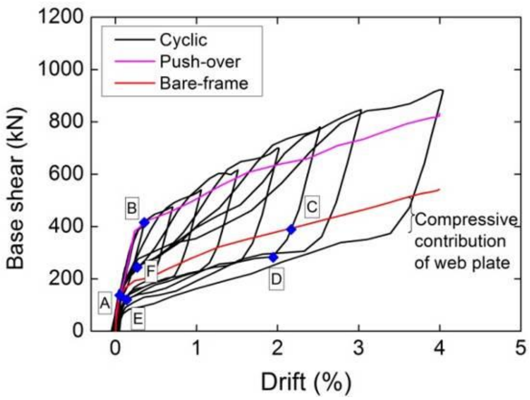

Fig. 5 – Significant points in SC-SPSW responses

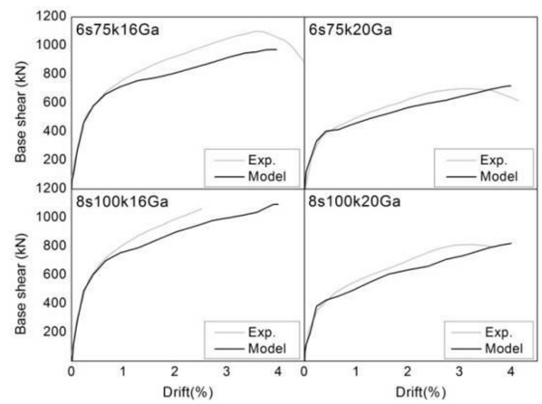

Fig. 6 – Comparison of model pushover curves and experimental skeleton curves

In Fig. 6, the numerical pushover curve was compared with the positive portion of the experimental skeleton curves for each specimen. The stiffness of the simulative curve closely matches the stiffness of experimental curve before the web plate yielding. After the web plate yielding, the hysteretic envelop of each specimen significantly exceed the pushover capacity curve because of the nature of the hardening exhibited by the web plate materials. And the extent of the hardening increases with the increasing thickness of web plate. This verifies that the hardening property defined in the material model significantly impact the web plate cyclic behavior, and the results in [12] also show that the isotropic hardening should be assumed for A1008 plate, which is applied in this study.

Then the results of the cyclic analysis were compared with the test data from the experiments in Fig. 7, showing the model responses are in good agreement with the experimental responses before the strength degradation occurs in experiments. Since the models can't simulate the system damage, the responses before the web plates damage were only compared and investigated. Fig. 7(b) shows the hysteretic envelops from the numerical analyses and the experimental responses. In the positive direction (the actuator pushes the model), the model accurately predicts the actual behavior, while in the negative direction the tests show a some premature softening near the yield point where the experimental curves dip under the simulated curves. It is due to the asymmetry introduced by the roller and the asymmetry is more easily detected in the numerical models, this then will be discussed in the PT connection behavior. For clarity, the numerical and experimental behavior for specimen 8s100k20Ga subjected to cycle at 2% drift only were compared in Fig. 8. The characteristics of the unloading and reloading behavior for a cycle prior to web plate tearing can be captured by comparing the key points of hysteretic curves. The figure indicates that the model overestimates the strength during reloading (Point F) and underestimates the web plate resistance during unloading (Point D). But the amounts of energy dissipation in the model and the test are approximate. The overestimation of the reloading strength isdue to that the isotropic hardening model was used in web plate strain hardening, minor damage in the web plate was not simulated in the models. Also, the residual drift of the model is underestimated, which indicates that the recentering capability of the system is overestimated, the reloading strength is overestimated. The underestimation of web plate unloading resistance is believed to be concerned with the underestimation of the web plate shear strength and substantially, the web plate compressive stress developments differ between the test and the model.

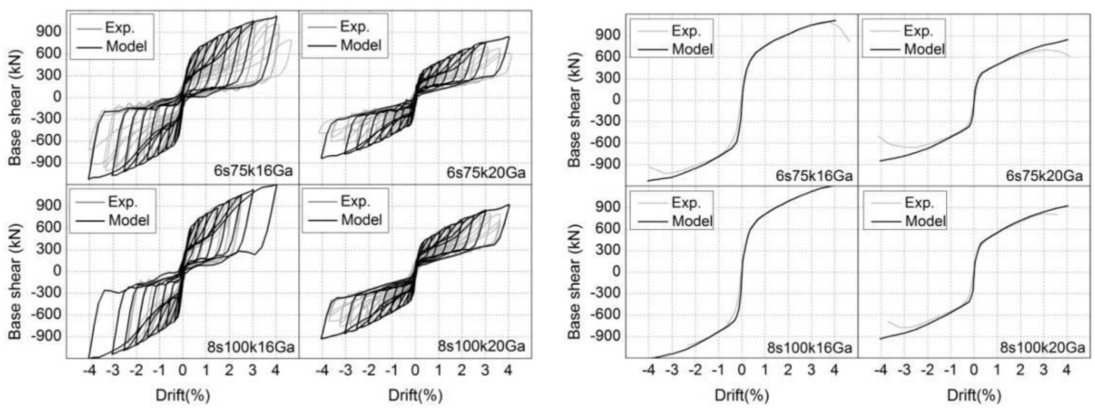

(a) (b)

Fig. 7 – Hysteretic responses of models and experiments: (a) Hysteretic curves and (b) Skeleton curves

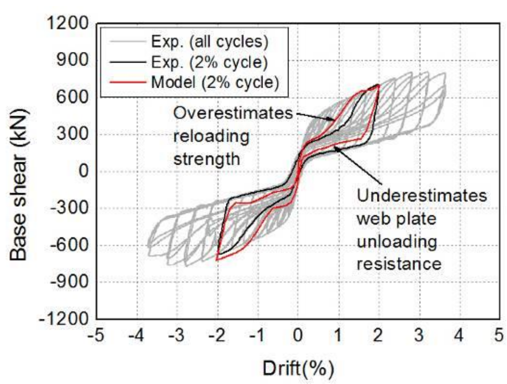

Fig. 8 – Comparison of experimental and numerical responses at 2% drift cycle of specimen 8s100k20Ga

3.2 PT Connection response

The recentering capability of the system correlates with the PT force response at HBE-to-VBE connection. Under the laterally loading, the response of the PT strands begins with initial prestress and the PT force increases linearly as the connection decompresses and the connection rotation increases. In Fig. 9, the cyclic responses of the PT strands at the middle HBE from the model and the test were compared, showing that the PT forces are slightly overestimated in the model. The PT stiffness is larger in the negative direction than that in the opposite direction, subsequently, it contributes to the system overall stiffness is larger, as shown in Fig. 7(b). In addition, some hysteretic area in the PT response is observed in model. As the PT strands and the boundary frame remain elastic under full loading, the hysteretic area is due to the slip at the roller rather than the yielding of the PT strands. It is also noted that the limited hysteretic area in the PT response at the positive direction is larger than that at the negative direction. This indicates that the roller introduces some asymmetry in the system and load path, and does have a minor influence on the demands on the north and south sides of the system. Meanwhile the amount of the hysteretic area increases for increasing the thickness of the web plate, showing that the web plate thickness effects the frame performance (e.g. in the numerical results the max slip for 8s100k16Ga is 27.4 mm and the max slip for 8s100k20Ga is 25.2 mm at 4% drift).

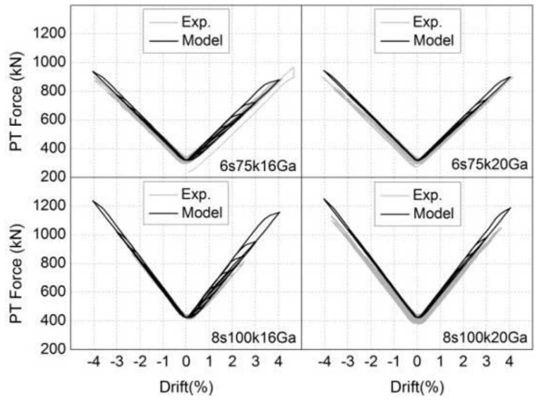

Fig. 9 – Comparison of PT forces at the middle HBE

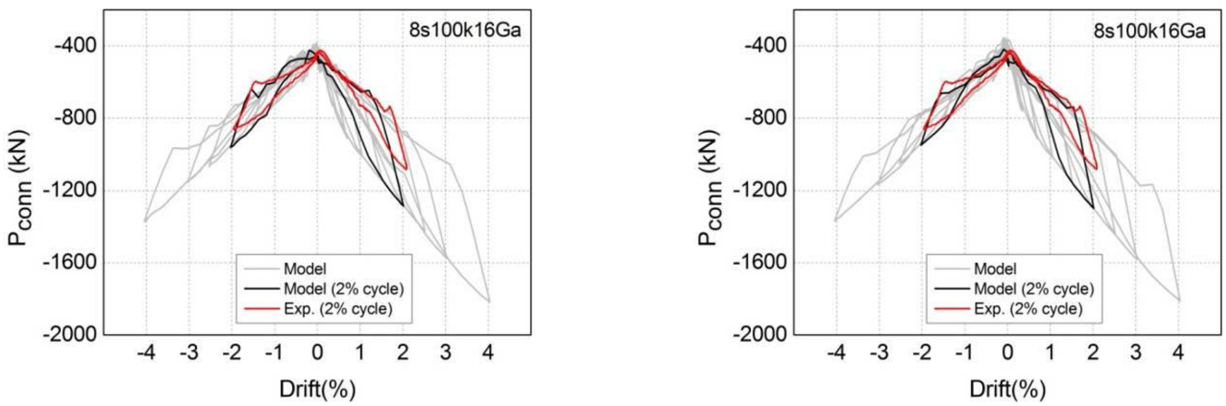

(a) (b)

Fig. 10 – Connection axial force demand (a) at north and (b) south connection for Specimen 8s100k16Ga

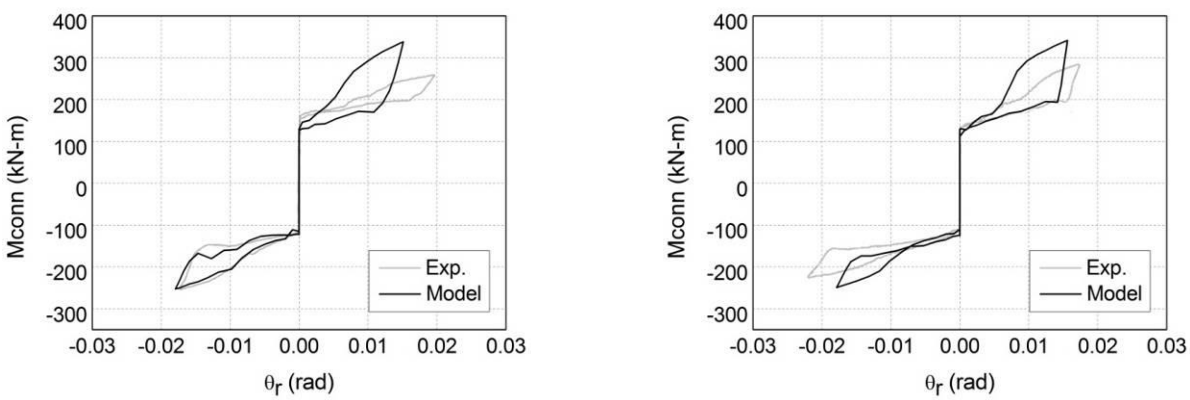

(a) (b)

Fig. 11 – Comparison of (a) north and (b) south connection moment response at the 2% drift cycle for Specimen 8s100k16Ga

The axial force and moment of the two ends of HBEs are able to be directly acquired by the modeling method proposed here using the contact forces between the ends of the HBE flange and the VBE flange face, subsequently, to determine the PT connection moment [2]. Assuming that the connection rocking point is the extreme fiber of the flange reinforcing plate, the relative rotation of the connection is attained from the output of the slot connector combined with cardan. For comparing with the experimental results in [5], Fig. 10 and Fig. 11 show the numerical and experimental comparisons of axial force and moment demands at 2% drift, respectively, for the north connection and the south connection in the middle HBE in specimen 8s100k16Ga. The responses of the both connections in the model overestimate the experimental measured responses, especially in the positive direction. Dowden et al. have presented that the axial force at HBE ends includes PT force (T_s), the pull-in force of the VBEs ($P_{HBE(VBE)}$) and the web plate force along the HBE ($P_{HBE(web)}$) in [2]. Thus, the overestimation in the connection axial demands is primarily believed to be due to the overestimation of the PT force, as shown in Fig. 9, and the overestimation of the web plate reloading strength, which results in the overestimation of $P_{HBE(VBE)}$ and $P_{HBE(web)}$. Similar to the axial force demand, the connection moment demands are also overestimated, shown in Fig. 11. Furthermore, the connection responses ($P_{conn}, M_{conn}, \theta_r$) are asymmetric.

Although the models overestimate the axial force and moment demands of the PT connection, the general trend of the PT connection behavior in the numerical simulation is consistent with the trend of the test results. If neglect the effect of the slip on the PT connection hysteretic response, the models are able to reasonably predict the PT connection behavior in SC-SPSW.

3.3 Web plate behavior

Web plate behaves as the energy dissipation component and contributes significant initial stiffness and strength for the SC-SPSW. It resists lateral load through tension field action and dissipate energy through yielding in the direction of the tension field. However, it should be noted that the web plates have some compressive strength that should be concerned in the design and the analysis of the SC-SPSW structures. Because it has an impact on lateral strength and the recentering capability of SC-SPSW. So the shell element model proposed here is applied to investigate the complex web plate behavior, such as the orientation of buckling waves in plates, the web plate stress and strain distribution.

As the SC-SPSW overall system response is a combination of the responses of PT boundary frame and the web plates. The web plate shear force resistance in the system is able to be equivalently attained by subtracting the bare frame shear force from the system base shear force. Fig. 12 compares the equivalent web plate shear force of the models and the experiments for each specimen, respectively. It is found that the web plate shear strength is underestimated after the web plates yielding, and the initial stiffness of the web plates is closely simulated. Models with thicker web plates are able to resist lager shear force under the lateral load. The extent of the shear strength underestimation is similar for the models with same thick web plates, and the web plate strength capabilities in models and experiments have an identical variation trend, shown in Fig. 13.

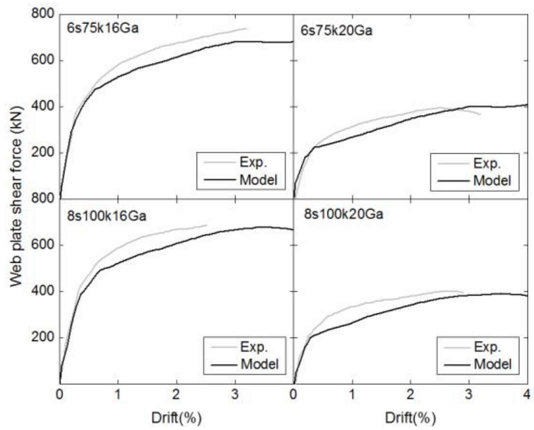

Fig. 12 – Comparison of web plate shear force resistance

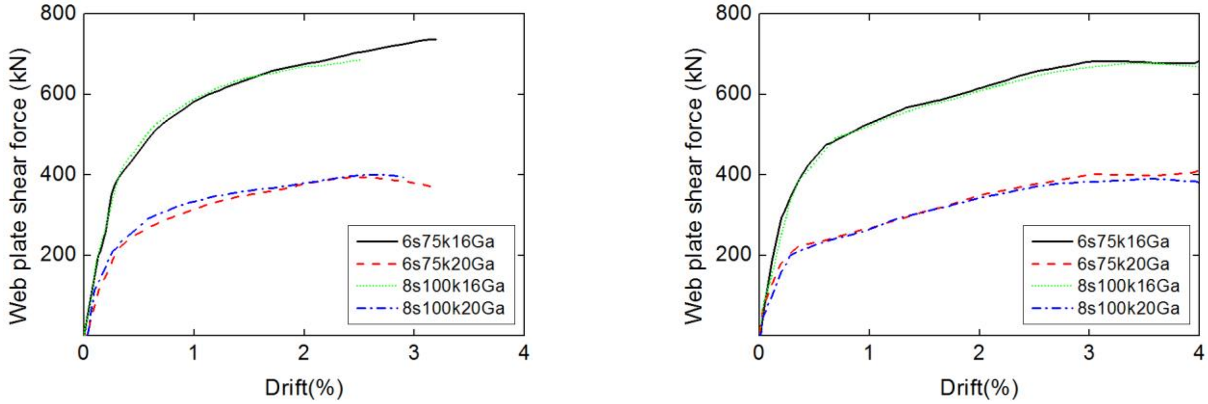

(a) (b)

Fig. 13 – Web plate shear resistance of (a) experiments and (b) models

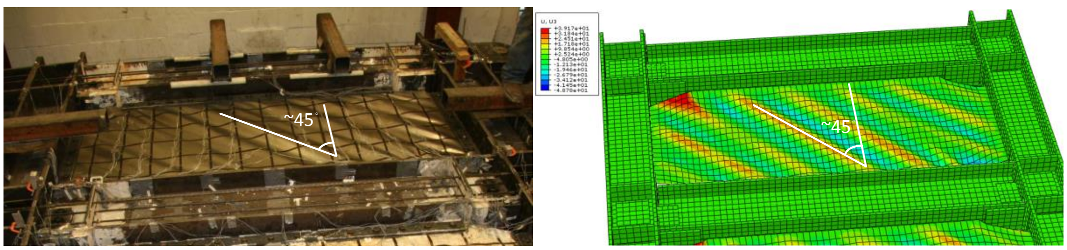

(a) (b)

Fig. 14 – Comparison of web plate responses at 2% drift in (a) experiment (b) shell element model for specimen 8s100k20Ga

About the discrepancy of the web plate behavior in the models and experiments, Fig. 14 shows an overview of buckling waves for specimen 8s100k20Ga at 2% drift. The number of the buckling waves in experiment reached 11, with the amplitude of the waves approximately 38 mm, whereas the number of the buckling waves in the model is 9, with the max amplitude of the waves about 40 mm. These differences result from that some phenomena (such as slips of the web plate corners at the fish plate connection, the web plate kinking and tearing near the corners) are not accurately simulated in the models, but they can have an effect on the whole web plate strain and stress distribution. Therefore, the experimental results demonstrate higher shear strength in the web plates as the tension field action better develops. With the web plate strength underestimation, the compressive strength in web plates also is underestimated, which results in the underestimation of the system unloading resistance for the cyclic behavior, seen in Fig. 8. Additionally, the orientation of the buckling waves from the vertical is about 45 degree both in the experiment and in the model, which is consistent with the assumed inclined angle.

3.4 Model evaluation

The SC-SPSW numerical responses including hysteresis behavior, PT connection responses, and web plate strength capability were analyzed and compared with the experimental results. It is verified that the numerical results are able to agree with the experimental performance. In general, the hysteresis behavior in model is well approximate with the experimental hysteresis and the models can be used to predict SC-SPSW performance before the web plate damage occurs. In particular, the model overestimates the reloading strength and underestimates the web plate shear and compressive strength during unloading. The PT force and the PT connection axial force and moment demands are overestimated due to the PT force losses are not simulated. While the web plate strength is underestimated, which is ascribed to the discrepancy of tension filed formation between the simulation and the actual behavior. Even so, the PT connection and web plate behavior variation trends keep consistent with the experimental responses, the model is appropriate for investigating the parametric study of the SC-SPSW, especially studying the details of the web plates behavior.

4. Parameric Analysis of SC-SPSW Responses

The design parameters including web plate thickness, t_w, number of PT strands, N_s, and total initial PT force, T_0, have been investigated in the quasi-static cyclic experiments [4, 5]. The results showed that the specimens with more PT strands and larger initial PT forces have lower residual drifts and, therefore, better recentering capabilities. The specimens with thicker web plates had larger strength and energy dissipation. Also the thicker web plate in the system induced worse recentering capability owing to the compression resistance of web plate during unloading. This influence was neglected in the SC-SPSW design method proposed by Clayton et al.[10]. Although the experiments can identify the effect that the web plate compression resistance has on the SC-SPSW performance, it is hard to be directly measured and quantified. Thus, the modeling method employed in this study is proposed to present the system detailed responses, such as the HBE axial force, the web plate stress and strain disstribution, which are significant but difficult to be directly captured in the experiments. The impacts of the varied parameters, t_w, N_s and T_0, on the SC-SPSW responses are explained.

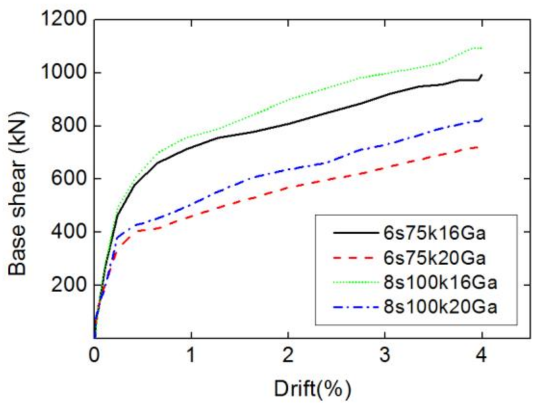

(a)

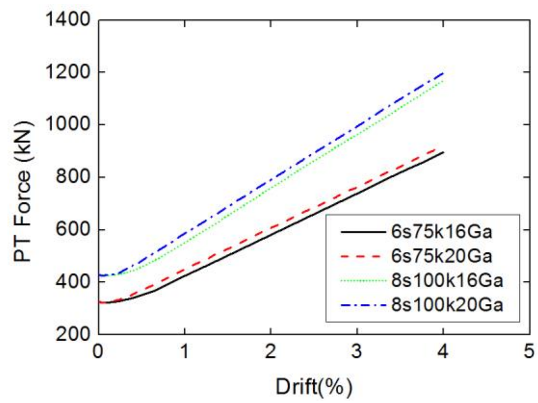

(b)

Fig. 15 – (a) Base shear versus drift response and (b) PT force versus drift response of the models under monotonic loading

Table 1 – Comparison of the system stiffness for the models

Models	K_1 **(kN/m)**	K_2 **(kN/m)**	K_3 **(kN/m)**
6s75k16Ga	48182	8428	2198
6s75k20Ga	34862	4453	2238
8s100k16Ga	51096	9061	2664
8s100k20Ga	38096	5851	2690

Fig. 15 shows the comparison of the model force-displacement responses under monotonic load. The values of the stiffness for the models are also caculated in Table 1. K_1 is the initial stiffness and is a combination of the elastic tension field stiffness of the web plate and the pre-decompression stiffness of the PT frame. K_2 is the system stiffness just after connection decompression and combines the elastic tension field stiffness with the decreased PT frame stiffness following decompression. K_3 is the combination of the post-decompression stiffness of the PT frame and the post-yield strain hardening stiffness of the web plate. It is found that increasing the number of PT strands increases the stiffness and strength of the system in full loading process. When the number of PT strands increases from 6 strands to 8 strands, K_1, K_2 and K_3 have an increase of about 6%, 7%, and 22%, respectively. This indicates that the effect of the PT strands on the initial stiffness is small and after the web plates yielding the number of PT strands variation in system response is noticeable. Additonally, When the web plate thickness increases from 20Ga (0.92 mm) to 16Ga (1.52 mm), K_1 has an increase of about 35%,

K_3 almost has no increase. It verifies that increasing the thickness of web plate significantly increases the system initial stiffness. Furthermore, from PT force versus drift responses of the models in Fig. 15(b), it is also found that the maganitude of the PT force is lower when the model has thicker web plate.

To show the effects of the parameters on the PT connection behavior, the connection moment (M_{conn}) versus rotation (θ_r) response for each model is shown in Fig. 16. Models with same number of PT strands decompress with the same connection moment. The connection moment increases for increasing the number of PT strands. While the PT force is slightly negatively affected by the web plate, increasing the web plate thickness results in the increasing of the connection moment, this implies the the PT boundary frame demands significantly correlate with the web plate properties. But the connection moment caculation method in [1] (that the total PT force (T_s) multiply half the HBE depth), do not consider this interaction. The figure also indicates that after the connection decompression, the PT connection stiffness varies with the variation of the thickness of the web plate, but after the web plate yielding, the effects eliminate.

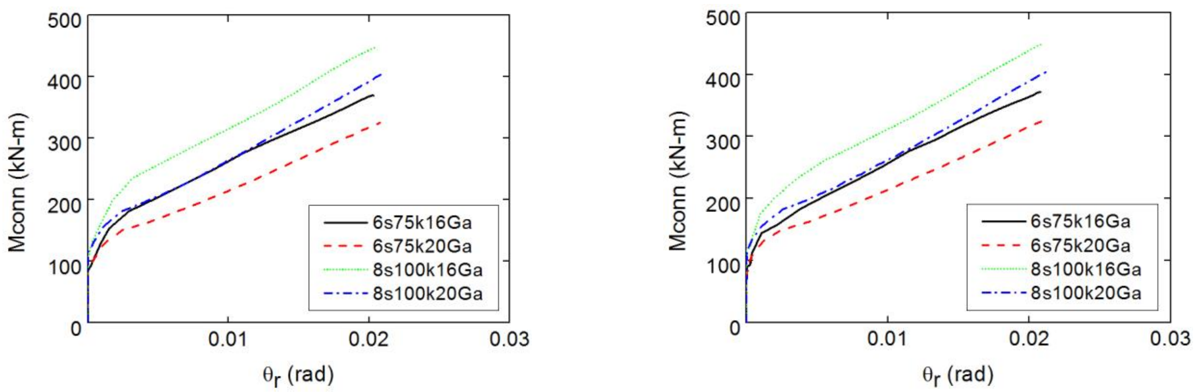

(a) (b)

Fig. 16 – Moments of (a) north and (b) south connection in the middle HBE of the models

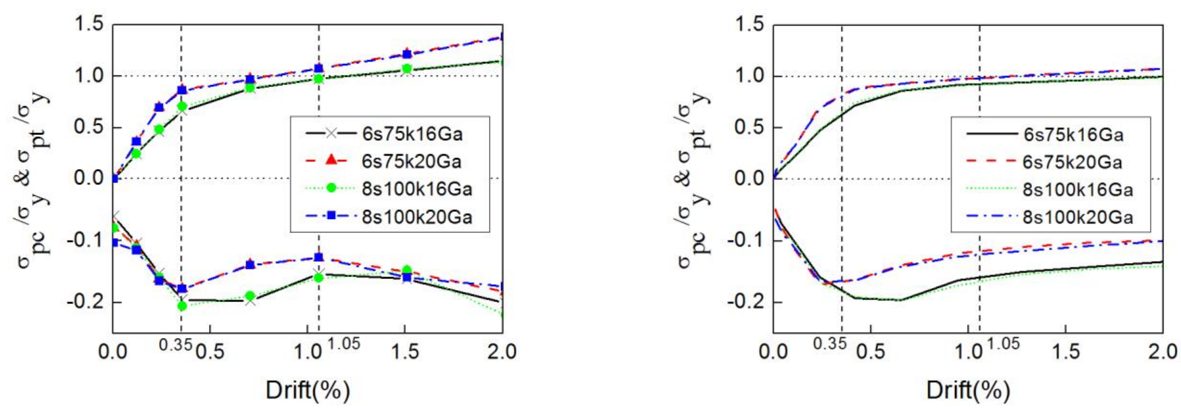

(a) (b)

Fig. 17 – Mean nominal principal stresses (σ_{pc} & σ_{pt}) normalized by plate nominal yield stress (σ_y) (a) under the cyclic load and (b) under the monotonic load

The web plate behavior is characterized by the tension field action and the experimental results have proved that there is non-negligible compressive strength in the web plate. The web plate principal stresses are easier extracted from the models relative to be measured through strain measurement in an experiment. The relative magnitudes of the mean principal tensile stress and mean principal compressive stress in the web plate under cyclic load and monotonic load, normalized by the plate yield strength are shown in Fig. 17. The principal stresses are plotted only at the peak of each half-cycle in Fig. 17(a). Reasonably the web plate tensile stress increases with the increasing drift. While the mean principal tensile stress in the thicker web plate is lower at the same drift level. It is attributed to that the thicker web plate has less strain.

Noted that the compressive stress of the web plate is approximately 10%-20% of the web plate tensile yield strength. This is identical with the experimental results in [4, 5]. Generally, the compressive stress in the web plates increases for increasing the web plate thickness, but its variation with the loading drift is complex. Upon the cyclic loading, the magnitude of the compressive stress increases other than from 0.35% to 1.05% drifts. Here drift 0.35% correspondes to the system yield drift, δ_y. The system yielding progressively occurs around 0.35% to 1.05% drifts. In this phase, the web plate compressive stresses are changing to tensile stresses. Therefore, the web plate compressive stress first increases with the increasing drift during the elastic phase, then decreases during yielding occurs progressively over the web plate. The changing trend before 1.05% drift under the cyclic load is similar with that under the monotonic load. However, after 1.05% drift, under the monotonic load the compressive stress continues to decrease, whereas under the cyclic load the trend turns to increase. This is thought to relate to the accumulated plastic strain of web plate, as shown in Fig. 18. 6s75k16Ga-M and 6s75k16Ga-C seperately identifies the models under monotonic load and cyclic load. The convention is also suitable to other models. It is found that the amount of the mean accumulated plastic strain near 1.05% drift under the cyclic load has exceeded the amount at 2% drift under the monotonic load. This indicates that when the web plate strain is large enough, the compressive stress would increase in order to stabilize the tension field buckling. It also indicates that web plate tension field action is more obvious under the cyclic load. In all, the web plate compressive strength tends to increase after the web plate full yielding, and its influence on the SC-SPSW hysteretic behavior will be significant, because it will increase the system energy dissipation and decrease the system self-centering capability.

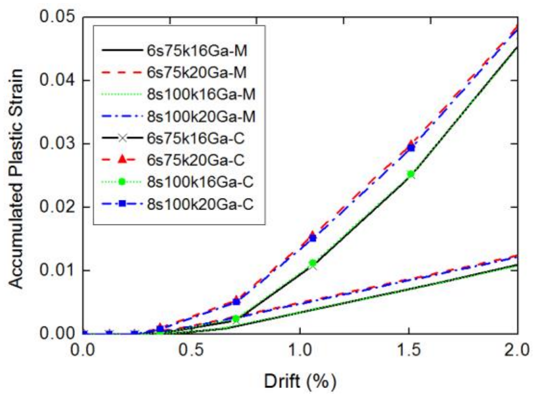

Fig. 18 – Accumulated plastic strain of web plates

5. Conclusions

Models of SC-SPSW using shell elements to simulate the web plate, solid elements to simulate the boundary frame were built in this study. The simulations showed a good agreement with the experimental results. The PT force was slightly overestimated, which resulted in the overestimation of the PT connenction axial force and moment responses in some extent. The web plate strength was underestimated as some web plate damage, which has effects on the tension field action, was not simulated in the models. Nonetheless, the model accurately predicted the stiffness and strength of the system before web plate damage occured. The variation in the system responses of the models were consistent with the experimental results when impacted by the various parameters. Except that, the complex behavior of PT connection and web plate were capable to directly acquired from the numerical models. This study provides an effcetive modeling method for the SC-SPSW parametric study in the future.

The effects on the model responses of the parameters: the number of PT strands at each HBE-to-VBE connection and the thickness of the web plates were also explained. The results showed that increasing the web plate thickness increased the PT boundary frame demands owing to the connection moment was affected by the web plate thickness. In addition to the web plate had a negatively impact on the PT force response, there was non-negligible compressive strength in the web plate. The compressive stress is higher in the thicker web plate. It is of more importance that the compressive strength in web plate is related to the accumulated plastic strain in web plate. As the accumulated plastic strain rapidly increases with the increasing of the drift under the cyclic load, the compressive stress else increases and its effects on the system seismic performance will be more noticeable. Further research is required to quantify the impacts of the parameters on the system responses.

6. References

[1] Clayton PM, Berman JW, Lowes LN (2012): Seismic design and performance of self-centering steel plate shear walls. *Journal of Structural Engineering*, **138** (1), 22-30.

[2] Dowden DM, Purba R, Bruneau M (2012): Behavior of self-centering steel plate shear walls and design considerations. *Journal of Structural Engineering*, **138** (1), 11-21.

[3] Clayton PM (2010): Self-centering steel plate shear walls: Development of design procedure and evaluation of seismic performance. *Master dissertation*, University of Washington, Seattle.

[4] Winkley TB (2011): Self-centering steel plate shear walls: Large scale experimental investigation. *Master dissertation*, University of Washington, Seattle.

[5] Clayton PM, Winkley TB, Berman JW, Lowes LN (2012): Experimental Investigation of Self-Centering Steel Plate Shear Walls. *Journal of Structural Engineering*, **138**, 952-960.

[6] Clayton PM , Dowden DM, Li C-H, Berman JW, Bruneau M, Lowes LN, Tsai K-C(2013): Full-Scale Testing of Self-Centering Steel Plate Shear Walls. *Structures Congress 2013*, 1694-1700.

[7] Clayton PM, Tsai C-Y, Berman JW, Lowes LN (2015): Comparison of web plate numerical models for self-centering steel plate shear walls. *Earthquake engineering and structural dynamics*, **44** (12), 2093-2110.

[8] Clayton PM, Winkley TB, Berman JW, Lowes LN, Dowden DM, Bruneau M (2012): Numerical and Experimental Studies of Self-Centering Steel Plate Shear Walls. *Proceedings of the 15th World Conference on Earthquake Engineering*, Lisbon.

[9] Clayton PM, Berman JW, Lowes LN (2013): Subassembly testing and modeling of self-centering steel plate shear walls. *Engineering Structures*, 1848-1857.

[10] Clayton PM, Berman JW, Lowes LN (2015): Seismic performance of self-centering steel plate shear walls with beam-only-connected web plates. *Journal of constructional steel research*, **106**, 198-208.

[11] Garlock MM, Sauce R, Ricles JM (2007): Behavior and design of posttensioned steel frame systems. *Journal of Structural Engineering*, **133** (3), 389-399.

[12] Webster DJ (2013): The inelastic seismic response of steel plate shear wall web plates and their interaction with the vertical boundary members. *PhD dissertation*, University of Washington, Seattle.